


**Observation of Photoassociation Resonances in Ultracold Atom-Molecule Collisions**

Jin Cao,<sup>1,2,\*</sup> Bo-Yuan Wang,<sup>1,2,\*</sup> Huan Yang<sup>①</sup>,<sup>1,2,3,\*</sup> Zhi-Jie Fan,<sup>1,2</sup> Zhen Su,<sup>1,2</sup> Jun Rui<sup>①</sup>,<sup>1,2,3</sup>  
Bo Zhao<sup>①</sup>,<sup>1,2,3</sup> and Jian-Wei Pan<sup>1,2,3</sup>

<sup>1</sup>*Hefei National Research Center for Physical Sciences at the Microscale and School of Physical Sciences, University of Science and Technology of China, Hefei 230026, China*

<sup>2</sup>*Shanghai Research Center for Quantum Science and CAS Center for Excellence in Quantum Information and Quantum Physics, University of Science and Technology of China, Shanghai 201315, China*

<sup>3</sup>*Hefei National Laboratory, University of Science and Technology of China, Hefei 230088, China*

 (Received 10 August 2023; revised 1 January 2024; accepted 8 February 2024; published 1 March 2024)

We report on the observation of photoassociation resonances in ultracold collisions between  $^{23}\text{Na}^{40}\text{K}$  molecules and  $^{40}\text{K}$  atoms. We perform photoassociation in a long-wavelength optical dipole trap to form deeply bound triatomic molecules in electronically excited states. The atom-molecule Feshbach resonance is used to enhance the free-bound Franck-Condon overlap. The photoassociation into well-defined quantum states of excited triatomic molecules is identified by observing resonantly enhanced loss features. These loss features depend on the polarization of the photoassociation lasers, allowing us to assign rotational quantum numbers. The observation of ultracold atom-molecule photoassociation resonances paves the way toward preparing ground-state triatomic molecules, provides a new high-resolution spectroscopy technique for polyatomic molecules, and is also important to atom-molecule Feshbach resonances.

DOI: [10.1103/PhysRevLett.132.093403](https://doi.org/10.1103/PhysRevLett.132.093403)

Photoassociation of ultracold atoms is a resonant light-assisted collision process, in which two colliding atoms absorb a photon and form an excited diatomic molecule [1–3]. Since the first experimental observation about three decades ago [4–6], photoassociation of ultracold atoms has made significant contributions to the study of ultracold atoms and molecules. For example, photoassociation is a general approach to forming molecules. In contrast to magnetoassociation, which forms extremely weakly bound halo molecules [7], photoassociation can form molecules in various rovibrational levels by tuning laser frequencies and using multiphoton processes [8–18]. In addition to forming molecules, photoassociation provides a new high-resolution molecular spectroscopy technique [1–6], which enables the study of high-lying states that are difficult to access for conventional molecular spectroscopy.

With the preparation of ultracold diatomic molecules [19–31], atom-atom photoassociation may be extended to atom-molecule photoassociation or molecule-molecule photoassociation. Such extensions will provide a new high-resolution spectroscopy technique for polyatomic molecules whose constituent atoms can be precooled. Photoassociation spectroscopy of polyatomic molecules can probe highly vibrationally excited molecular states, which are difficult to measure using conventional methods that start from the equilibrium configuration [2,3]. Such extensions also provide a general approach to preparing ultracold polyatomic molecules. Compared to diatomic molecules, polyatomic molecules have more degrees of

freedom for control and offer many new research opportunities [32–34]. For example, ultracold triatomic molecules present an ideal quantum system to study the notoriously difficult quantum-mechanical three-body problem [35,36]. Symmetric top polyatomic molecules possess nearly degenerate doublet states with opposite parity. The dipole moment of an asymmetric top molecule may have projections along more than one principal axis. Moreover, asymmetric top molecules consisting of four atoms can have chirality. These new features make polyatomic molecules potentially useful in quantum simulations of novel spin Hamiltonians and precision measurements in fundamental physics [37–39].

Extending the photoassociation from a diatomic system to a polyatomic system has been proposed since about two decades ago [2,3]. However, the complexity of polyatomic molecules makes such extensions extremely challenging. Recently, the prospects of ultracold photoassociation in atom-molecule collisions [40–44] or molecule-molecule collisions [45] have been theoretically studied. Because the short-range interactions are very complicated, only the long-range polyatomic states near the dissociation limit can be studied. However, the density of states of these high-lying polyatomic molecular states is very high due to the heavy mass of atoms and their strongly anisotropic interactions [46,47]. Consequently, it is unclear whether photoassociation will result in well-resolved resonant features or a broad quasicontinuous profile containing numerous unresolvable resonances [41,43]. Another major obstacle

to the observation of photoassociation resonances is that the trapping laser can excite the polyatomic collision complex with a high excitation rate [48–51]. This process contributes to a background loss and, thus, may hinder the possibility of photoassociation into well-defined quantum states of polyatomic molecules.

In this Letter, we report on the observation of photoassociation resonances in ultracold collisions between  $^{23}\text{Na}^{40}\text{K}$  molecules and  $^{40}\text{K}$  atoms in a long-wavelength optical dipole trap. To overcome the difficulty caused by the high density of states, we use Feshbach-enhanced photoassociation [52,53] to form deeply bound triatomic molecules in electronically excited states. We identify the photoassociation of  $^{23}\text{Na}^{40}\text{K}$  molecules and  $^{40}\text{K}$  atoms into well-defined quantum states of excited triatomic molecules by observing resonantly enhanced loss features. The loss features depend on the polarization of the photoassociation lasers, allowing us to assign the rotational quantum number of the triatomic molecular states.

Our experiment starts with the preparation of an ultracold mixture of  $^{23}\text{Na}^{40}\text{K}$  molecules and  $^{40}\text{K}$  atoms in a long-wavelength optical dipole trap. The experimental procedures are given in Supplemental Material [54]. In brief, we first create a deeply degenerate atomic mixture of  $^{23}\text{Na}$  and  $^{40}\text{K}$  atoms with a large number imbalance in a large-volume optical dipole trap at a wavelength of 1064 nm [31]. We then load the atoms into a long-wavelength crossed-beam optical dipole trap formed by two laser beams. The wavelengths of the two trapping beams are 1558 and 1583 nm, respectively. The horizontal trapping beam propagates along the direction of the magnetic field, and the vertical trapping beam propagates perpendicular to the direction of the magnetic field. After loading the atomic mixture into the long-wavelength optical dipole trap, we create  $^{23}\text{Na}^{40}\text{K}$  Feshbach molecules at 77.6 G by magneto-association and then transfer them into the rovibrational ground state by stimulated Raman adiabatic passage. After removing the  $^{23}\text{Na}$  atoms by a resonant light pulse, we obtain an ultracold mixture of  $^{23}\text{Na}^{40}\text{K}$  molecules and  $^{40}\text{K}$  atoms. The  $^{23}\text{Na}^{40}\text{K}$  molecules are prepared in the hyperfine level  $|v, n, m_{\text{Na}}, m_{\text{K}}\rangle = |0, 0, -3/2, -4\rangle$ , where  $v$  and  $n$  represent the vibrational and rotational quantum numbers, respectively, and  $m_{\text{Na}}$  and  $m_{\text{K}}$  represent the projections of the nuclear spins. The  $^{40}\text{K}$  atoms are in the lowest hyperfine state  $|f, m_f\rangle_{\text{K}} = |9/2, -9/2\rangle$ . The number of  $^{40}\text{K}$  atoms is about one order of magnitude larger than the number of  $^{23}\text{Na}^{40}\text{K}$  molecules.

We use the horizontal trapping laser as the photoassociation laser. The experimental scheme is illustrated in Fig. 1. The 1558 and 1583 nm photoassociation lasers may form deeply bound excited molecules below the  $\text{NaK}(b^3\Pi) + \text{K}(4^2\text{S})$  dissociation limit with binding energies of about  $5100\text{ cm}^{-1}$ . The density of states of these deeply bound states is much lower than that of high-lying states near the dissociation limit, and, thus, there may exist

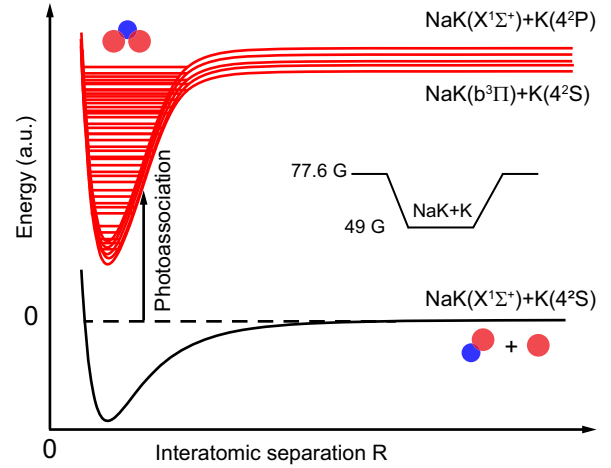


FIG. 1. Illustration of photoassociation in ultracold collisions between  $^{23}\text{Na}^{40}\text{K}$  molecules and  $^{40}\text{K}$  atoms. The ultracold  $^{23}\text{Na}^{40}\text{K}$  molecule and  $^{40}\text{K}$  atom absorb a photon and form a triatomic molecule in the electronically excited state if the laser frequency is in resonance with a free-bound transition. To suppress the photoexcitation of the collision complex by the trapping laser and to avoid the high density of states near the dissociation limit, we perform photoassociation to form deeply bound excited molecules in a long-wavelength optical dipole trap. To enhance the free-bound Franck-Condon overlap, photoassociation is performed in the vicinity of the atom-molecule Feshbach resonance by ramping the magnetic field to about 49 G, which is slightly above the resonance located at about 48.2 G.

well-resolved triatomic molecules that can be addressed by photoassociation. To enhance the Franck-Condon overlap, we study photoassociation in the vicinity of an atom-molecule Feshbach resonance located at about 48.2 G [60]. This is a resonance in  $s$ -wave scattering and has been carefully studied in previous works [34,61]. After preparing the atom-molecule mixture at a magnetic field of 77.6 G, we ramp the magnetic field to about 49 G, which is slightly higher than the resonance position. We hold the  $^{23}\text{Na}^{40}\text{K}$  molecules and  $^{40}\text{K}$  atoms for a certain time and then remove the  $^{40}\text{K}$  atoms using a resonant light pulse. After that, we ramp the magnetic field back to 77.6 G and measure the number of remaining  $^{23}\text{Na}^{40}\text{K}$  molecules by transferring them into Feshbach states for detection.

During the hold time, the inelastic collisions between  $^{23}\text{Na}^{40}\text{K}$  molecules and  $^{40}\text{K}$  atoms lead to the loss of  $^{23}\text{Na}^{40}\text{K}$  molecules. We change the frequency of the horizontal trapping laser and use the decay of the  $^{23}\text{Na}^{40}\text{K}$  molecules as a probe of the photoassociation. If the trapping laser frequency is in resonance with a free-bound transition, a pair of a  $^{23}\text{Na}^{40}\text{K}$  molecule and a  $^{40}\text{K}$  atom will absorb a photon and form an excited triatomic molecule, which will decay due to spontaneous emission. Consequently, the decay of  $^{23}\text{Na}^{40}\text{K}$  molecules will be resonantly enhanced. Therefore, the photoassociation into a well-defined quantum state of triatomic molecules will manifest itself as a resonantly enhanced loss feature.

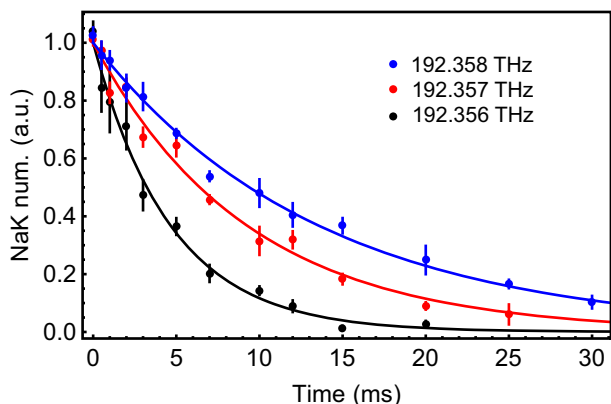


FIG. 2. The decay of the  $^{23}\text{Na}^{40}\text{K}$  molecule number in the atom-molecule mixture for different photoassociation laser frequencies. The time evolution of the  $^{23}\text{Na}^{40}\text{K}$  molecule number is recorded for different photoassociation laser frequency. The 1558 nm trapping laser is used as the photoassociation laser, the polarization of which is set to  $\sigma^+$ . The solid lines are exponential fits to the data with  $1/e$  lifetimes of 13.6(5) ms at 192.358 THz, 9.3(6) ms at 192.357 THz, and 4.7(3) ms at 192.356 THz. Each point represents the average of 3–5 measurements, and error bars represent the standard error of the mean.

To observe the resonant loss feature, the enhanced loss caused by the photoassociation resonances must be larger than the background loss. In the vicinity of the atom-molecule Feshbach resonance, the decay of the  $^{23}\text{Na}^{40}\text{K}$  molecules is greatly enhanced. At about 49 G, the typical lifetime of the  $^{23}\text{Na}^{40}\text{K}$  molecules in the atom-molecule mixture in the long-wavelength optical dipole trap is about 10 ms. One major contribution of the background loss may be caused by photoexcitation by the trapping laser [48,51]. In Ref. [34], we have observed that the triatomic Feshbach molecules can be quickly depleted by the 1064 nm trapping laser, which indicates the background loss near the Feshbach resonance may also be caused by the trapping laser. Although it is proposed that a long-wavelength optical dipole trap may be helpful to suppress the background losses [48], it is unclear whether this suppression is sufficient for observing resonant features. In our experiment, we first carefully study the decay of  $^{23}\text{Na}^{40}\text{K}$  molecules at different photoassociation laser frequencies. We find that in some frequency regions the decay rate of the  $^{23}\text{Na}^{40}\text{K}$  molecules can be enhanced by a factor of about 3 by varying the laser frequency. An example of such an enhanced loss is shown in Fig. 2, where the 1558 nm laser is used as the photoassociation laser. The decay rate of the  $^{23}\text{Na}^{40}\text{K}$  molecules at 192.356 THz (near a photoassociation resonance) is approximately 3 times larger than the decay rate at 192.358 THz (far away from a photoassociation resonance). We have checked that the decay rate near the resonance scales linearly with the atomic density (see Supplemental Material [54]). Therefore, we attribute such an enhanced loss to the photoassociation of  $^{23}\text{Na}^{40}\text{K}$

molecules and  $^{40}\text{K}$  atoms into a well-defined quantum state of triatomic molecules.

To search for more resonant loss features in a large frequency range, we record the number of remaining  $^{23}\text{Na}^{40}\text{K}$  molecules for a fixed hold time of 10 ms as a function of the horizontal trapping beam frequency, normalized to that for a zero hold time. The polarization of the horizontal trapping beam is set to either  $\sigma^+$  or  $\sigma^-$ . We first use the 1558 nm laser as the photoassociation laser to search in the frequency range between 192.35 and 192.42 THz. We then exchange the two trapping lasers and use the 1583 nm laser as the photoassociation laser to search in the range between 189.33 and 189.42 THz. In total, ten resonantly enhanced loss features are observed. We find that these loss features are dominantly excited by either  $\sigma^+$  or  $\sigma^-$  polarizations of the photoassociation laser. However, these loss features are not observed in a pure molecular gas. For the measurements in a pure molecular gas,

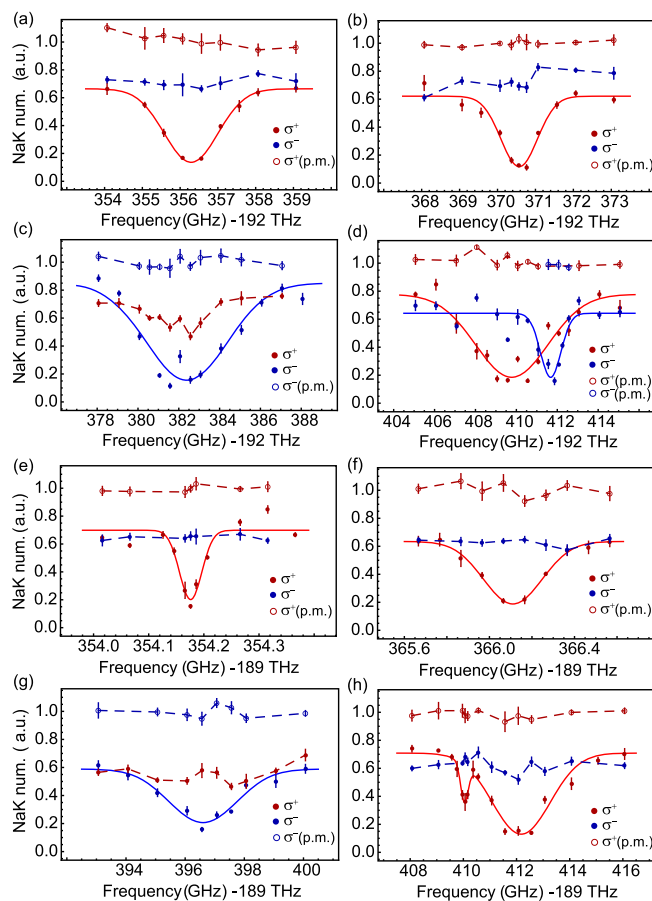


FIG. 3. The remaining number of  $^{23}\text{Na}^{40}\text{K}$  molecules is plotted as a function of the frequency of the photoassociation laser. Each loss feature is dominantly excited by either  $\sigma^+$  or  $\sigma^-$  polarization. For comparison, the data points for both the polarizations and the results for pure molecules (p.m.) are shown. The solid lines are Gaussian fits to the loss features. The dashed lines are guides to the eye. Each point represents the average of 3–5 measurements, and error bars represent the standard error of the mean.

TABLE I. The central frequencies and widths are obtained by Gaussian fits to the resonant loss features. The polarization of the photoassociation light is either  $\sigma^+$  or  $\sigma^-$ .

	Frequency (THz)	Width (GHz)	Polarization
1	192.3563	1.0	$\sigma^+$
2	192.3706	0.68	$\sigma^+$
3	192.3824	2.8	$\sigma^-$
4	192.4098	2.5	$\sigma^+$
5	192.4117	0.71	$\sigma^-$
6	189.354 18	0.03	$\sigma^+$
7	189.3661	0.19	$\sigma^+$
8	189.3966	1.6	$\sigma^-$
9	189.4100	0.20	$\sigma^+$
10	189.4122	1.5	$\sigma^+$

gas, the atoms are removed immediately after preparing the molecules. The comparison of different polarizations and the results for pure molecules are shown in Fig. 3. The dependence on the polarization of the photoassociation laser indicates that these resonant loss features represent rotationally resolved molecules. The data are fit to Gaussian functions. The center frequencies and the widths obtained by Gaussian fits are given in Table I. The loss feature located at 189.354 18 THz has a width of about 30 MHz, which is much narrower than other observed loss features.

These well-resolved loss features represent the photoassociation of  $^{23}\text{Na}^{40}\text{K}$  molecules and  $^{40}\text{K}$  atoms into well-defined quantum states of  $^{23}\text{Na}^{40}\text{K}_2$  molecules in electronically excited states. To gain further understanding of these molecular states, we calculate the energy of the equilibrium geometries of the doublet electronic excited states of  $^{23}\text{Na}^{40}\text{K}_2$  molecules using *ab initio* calculations [54]. These equilibrium geometries correspond to the local minimum of the three-dimensional potential energy surface. The energies of the lowest four equilibrium geometries above the  $\text{NaK}(X^1\Sigma^+) + \text{K}(4^2S)$  dissociation limit are shown in Fig. 4. The  $3^2A_1$ ,  $2^2B_1$ , and  $1^2B_2$  states have the  $C_{2v}$  symmetry, while the  $3^2A'$  state has the  $C_s$  symmetry. The molecular states observed in our experiment are lower in energy than the  $3^2A_1$  and  $2^2B_1$  states, while they are higher than the  $1^2B_2$  and  $3^2A'$  states by about 2800 and 1200  $\text{cm}^{-1}$ , respectively. Therefore, these molecular states may be considered as the vibrationally excited states of the  $1^2B_2$  and  $3^2A'$  states. Assuming that the potential energy surface near the minimum can be approximated by harmonic oscillators, the vibrational frequencies of the three normal modes of the  $1^2B_2$  and  $3^2A'$  states are calculated to be  $(v_1, v_2, v_3) = (120.0, 104.4, 68.8)$  and  $(92.0, 78.5, 47.3)$   $\text{cm}^{-1}$ , respectively. The energy of a vibrationally excited state may be given by  $E = n_1v_1 + n_2v_2 + n_3v_3$ , where  $n_1$ ,  $n_2$ , and  $n_3$  are the quantum numbers of the three normal modes. The cumulative number of vibrational levels against their energy

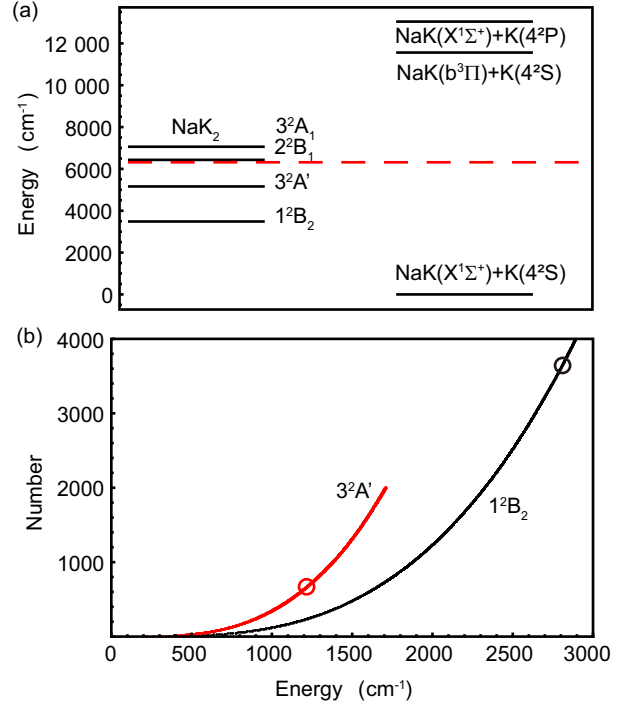


FIG. 4. The energy of the equilibrium geometries of the doublet states of  $^{23}\text{Na}^{40}\text{K}_2$  molecules. (a) The four lowest equilibrium geometries above the  $\text{NaK}(X^1\Sigma^+) + \text{K}(4^2S)$  dissociation limit obtained by *ab initio* calculations. The energy of the atom-diatomic molecule dissociation limit is also shown. The red dashed line represents the spectral region studied in the current experiment. (b) The cumulative number of vibrational states as a function of their energy for the  $1^2B_2$  and  $3^2A'$  states. The density of states is given by the gradient. The spectral regions in the current experiment are marked by circles.

can be counted, and the result is plotted in Fig. 4. Below the spectral region studied in our experiment, there are about 3600 and 600 vibrational levels for the  $1^2B_2$  and  $3^2A'$  states, respectively. The number of states will be larger if the anharmonicity of the potential is considered. For such high-lying states, the assignment of the vibrational quantum numbers for individual molecular states is difficult. We may still compare the density of states which is given by the gradient of the curve. The density of states near the spectral region studied in our experiment is about 4 and 1 per  $\text{cm}^{-1}$  for the  $1^2B_2$  and  $3^2A'$  states, respectively. The estimated density of states is higher than that observed in the experiment, which indicates that some molecular states are not observed, probably because they are very narrow or the Franck-Condon overlap is low.

Although the exact vibrational quantum numbers cannot be assigned due to the high density of states, the dependence on the polarization of the photoassociation laser may allow us to assign the rotational quantum numbers. For photoassociation of the atoms and diatomic molecules in the maximally polarized states, the nuclear spins may be neglected. The total angular momentum  $J = N + S$  of

triatomic molecules may be approximately a good quantum number, where  $N$  is the rotational quantum number and  $S$  is the electron spin [60]. The initial scattering state has a total angular momentum  $J = n + l + S = 1/2$  and the projection along the magnetic field is  $M_J = -1/2$ , where  $n = 0$  represents the rotational quantum number of  $^{23}\text{Na}^{40}\text{K}$  molecules,  $l = 0$  is the angular momentum of relative motion, and  $S = 1/2$  is the electron spin of  $^{40}\text{K}$  atoms. According to the selection rule of electronic dipole transitions  $\Delta J = 0, \pm 1$ , the total angular momentum of the excited molecules may be described by  $J' = 1/2$  or  $3/2$ . Because the initial state has  $M_J = -1/2$ , only  $\sigma^+$  transitions are allowed to final states with  $J' = 1/2$ , while  $\sigma^-$  transitions are forbidden. If  $J' = 3/2$ , then both transitions are allowed. Therefore, the molecular states that are dominantly excited by  $\sigma^-$  light may have a rotational quantum number  $J' = 3/2$ , and the molecular states that are dominantly excited by  $\sigma^+$  light may have a rotational quantum number  $J' = 1/2, 3/2$ .

In conclusion, we have observed photoassociation resonances in ultracold collisions between  $^{23}\text{Na}^{40}\text{K}$  molecules and  $^{40}\text{K}$  atoms. The photoassociation of atoms and molecules provides a new high-resolution spectroscopy technique for triatomic molecules. Moreover, our Letter opens up an avenue toward the preparation of ultracold deeply bound triatomic molecules in their electronic ground state. To this end, two-photon photoassociation or coherent transfer has to be developed to transfer triatomic molecules to the ground state. The well-resolved molecular states probed by one-photon photoassociation can serve as intermediate states for two-photon photoassociation or coherent transfer. Besides, the suppression of background loss near the atom-molecule Feshbach resonance [62,63] by using a long-wavelength optical trap will make the Feshbach resonance a powerful tool to study strongly interacting quantum gases.

We thank Feng Zhang for helpful discussions. This work was supported by the National Natural Science Foundation of China (under Grants No. 12241409, No. 12325407, and No. 12274393), the National Key R&D Program of China (under Grant No. 2018YFA0306502), the Chinese Academy of Sciences, the Anhui Initiative in Quantum Information Technologies, the Shanghai Municipal Science and Technology Major Project (Grant No. 2019SHZDZX01), and the Innovation Program for Quantum Science and Technology (Grant No. 2021ZD0302101).

\*These authors contributed equally to this work.

- [1] P. D. Lett, P. S. Julienne, and W. D. Phillips, *Annu. Rev. Phys. Chem.* **46**, 423 (1995).  
 [2] W. C. Stwalley and H. Wang, *J. Mol. Spectrosc.* **195**, 194 (1999).

- [3] K. M. Jones, E. Tiesinga, P. D. Lett, and P. S. Julienne, *Rev. Mod. Phys.* **78**, 483 (2006).  
 [4] H. R. Thorsheim, J. Weiner, and P. S. Julienne, *Phys. Rev. Lett.* **58**, 2420 (1987).  
 [5] P. D. Lett, K. Helmerson, W. D. Phillips, L. P. Ratliff, S. L. Rolston, and M. E. Wagshul, *Phys. Rev. Lett.* **71**, 2200 (1993).  
 [6] J. D. Miller, R. A. Cline, and D. J. Heinzen, *Phys. Rev. Lett.* **71**, 2204 (1993).  
 [7] T. Köhler, K. Góral, and P. S. Julienne, *Rev. Mod. Phys.* **78**, 1311 (2006).  
 [8] A. Fioretti, D. Comparat, A. Crubellier, O. Dulieu, F. Masnou-Seeuws, and P. Pillet, *Phys. Rev. Lett.* **80**, 4402 (1998).  
 [9] C. Gabbanini, A. Fioretti, A. Lucchesini, S. Gozzini, and M. Mazzoni, *Phys. Rev. Lett.* **84**, 2814 (2000).  
 [10] D. Wang, J. Qi, M. F. Stone, O. Nikolayeva, H. Wang, B. Hattaway, S. D. Gensemer, P. L. Gould, E. E. Eyler, and W. C. Stwalley, *Phys. Rev. Lett.* **93**, 243005 (2004).  
 [11] M. W. Mancini, G. D. Telles, A. R. L. Caires, V. S. Bagnato, and L. G. Marcassa, *Phys. Rev. Lett.* **92**, 133203 (2004).  
 [12] J. M. Sage, S. Sainis, T. Bergeman, and D. DeMille, *Phys. Rev. Lett.* **94**, 203001 (2005).  
 [13] J. Deiglmayr, A. Grochola, M. Repp, K. Mörtlbauer, C. Glück, J. Lange, O. Dulieu, R. Wester, and M. Weidemüller, *Phys. Rev. Lett.* **101**, 133004 (2008).  
 [14] K. Aikawa, D. Akamatsu, M. Hayashi, K. Oasa, J. Kobayashi, P. Naidon, T. Kishimoto, M. Ueda, and S. Inouye, *Phys. Rev. Lett.* **105**, 203001 (2010).  
 [15] G. Reinaudi, C. B. Osborn, M. McDonald, S. Kotochigova, and T. Zelevinsky, *Phys. Rev. Lett.* **109**, 115303 (2012).  
 [16] R. Wynar, R. S. Freeland, D. J. Han, C. Ryu, and D. J. Heinzen, *Science* **287**, 1016 (2000).  
 [17] V. Bendkowsky, B. Butscher, J. Nipper, R. L. James, P. Shaffer and, and T. Pfau, *Nature (London)* **458**, 1005 (2009).  
 [18] S. Hollerith, J. Zeiher, J. Rui, A. Rubio-Abadal, V. Walther, T. Pohl, D. M. Stamper-Kurn, I. Bloch, and C. Gross, *Science* **364**, 664 (2019).  
 [19] K.-K. Ni, S. Ospelkaus, M. H. G. de Miranda, A. Pe'er, B. Neyenhuis, J. J. Zirbel, S. Kotochigova, P. S. Julienne, D. S. Jin, and J. Ye, *Science* **322**, 231 (2008).  
 [20] P. K. Molony, P. D. Gregory, Z. Ji, B. Lu, M. P. Köppinger, C. R. Le Sueur, C. L. Blackley, J. M. Hutson, and S. L. Cornish, *Phys. Rev. Lett.* **113**, 255301 (2014).  
 [21] T. Takekoshi, L. Reichsöllner, A. Schindewolf, J. M. Hutson, C. R. Le Sueur, O. Dulieu, F. Ferlaino, R. Grimm, and H.-C. Nägerl, *Phys. Rev. Lett.* **113**, 205301 (2014).  
 [22] J. W. Park, S. A. Will, and M. W. Zwierlein, *Phys. Rev. Lett.* **114**, 205302 (2015).  
 [23] M. Guo, B. Zhu, B. Lu, X. Ye, F. Wang, R. Vexiau, N. Bouloufa-Maafa, G. Quémener, O. Dulieu, and D. Wang, *Phys. Rev. Lett.* **116**, 205303 (2016).  
 [24] T. M. Rvachov, H. Son, A. T. Sommer, S. Ebadi, J. J. Park, M. W. Zwierlein, W. Ketterle, and A. O. Jamison, *Phys. Rev. Lett.* **119**, 143001 (2017).  
 [25] K. K. Voges, P. Gersema, M. Meyer zum Alten Borgloh, T. A. Schulze, T. Hartmann, A. Zenesini, and S. Ospelkaus, *Phys. Rev. Lett.* **125**, 083401 (2020).  
 [26] I. Stevenson, A. Z. Lam, N. Bigagli, C. Warner, W. Yuan, S. Zhang, and S. Will, *Phys. Rev. Lett.* **130**, 113002 (2023).

- [27] L. R. Liu, J. D. Hood, Y. Yu, J. T. Zhang, N. R. Hutzler, T. Rosenband, and K.-K. Ni, *Science* **360**, 900 (2018).
- [28] X. He, K. Wang, J. Zhuang, P. Xu, X. Gao, R. Guo, C. Sheng, M. Liu, J. Wang, J. Li *et al.*, *Science* **370**, 331 (2020).
- [29] L. DeMarco, G. Valtolina, K. Matsuda, W. G. Tobias, J. P. Covey, and J. Ye, *Science* **363**, 853 (2019).
- [30] A. Schindewolf, R. Bause, X.-Y. Chen, M. Duda, T. Karman, I. Bloch, and X.-Y. Luo, *Nature (London)* **607**, 677 (2022).
- [31] J. Cao, H. Yang, Z. Su, X.-Y. Wang, J. Rui, B. Zhao, and J.-W. Pan, *Phys. Rev. A* **107**, 013307 (2023).
- [32] M. Zeppenfeld, B. G. U. Englert, R. Glöckner, A. Prehn, M. Mielenz, C. Sommer, L. D. van Buuren, M. Motsch, and G. Rempe, *Nature (London)* **491**, 570 (2012).
- [33] D. Mitra, N. B. Vilas, C. Hallas, L. Anderegg, B. L. Augenbraun, L. Baum, C. Miller, S. Raval, and J. M. Doyle, *Science* **369**, 1366 (2020).
- [34] H. Yang, J. Cao, Z. Su, J. Rui, B. Zhao, and J.-W. Pan, *Science* **378**, 1009 (2022).
- [35] T. Kraemer, M. Mark, P. Waldburger, J. G. Danzl, C. Chin, B. Engeser, A. D. Lange, K. Pilch, A. Jaakkola, H.-C. Nägerl *et al.*, *Nature (London)* **440**, 315 (2006).
- [36] T. Lompe, T. B. Ottenstein, F. Serwane, A. N. Wenz, G. Zrn, and S. Jochim, *Science* **330**, 940 (2010).
- [37] M. L. Wall, K. Maeda, and L. D. Carr, *New J. Phys.* **17**, 025001 (2015).
- [38] P. Yu and N. R. Hutzler, *Phys. Rev. Lett.* **126**, 023003 (2021).
- [39] B. L. Augenbraun, J. M. Doyle, T. Zelevinsky, and I. Kozyryev, *Phys. Rev. X* **10**, 031022 (2020).
- [40] M. Lepers, O. Dulieu, and V. Kokoouline, *Phys. Rev. A* **82**, 042711 (2010).
- [41] J. Pérez-Ríos, M. Lepers, and O. Dulieu, *Phys. Rev. Lett.* **115**, 073201 (2015).
- [42] J. Schnabel, T. Kampschulte, S. Rupp, J. Hecker Denschlag, and A. Köhn, *Phys. Rev. A* **103**, 022820 (2021).
- [43] B. Shammout, L. Karpa, S. Ospelkaus, E. Tiemann, and O. Dulieu, *J. Phys. Chem. A* **127**, 7872 (2023).
- [44] A. A. Elkamshishy and C. H. Greene, *J. Phys. Chem. A* **127**, 18 (2023).
- [45] M. Gacesa, J. N. Byrd, J. Smucker, J. A. Montgomery, and R. Côté, *Phys. Rev. Res.* **3**, 023163 (2021).
- [46] M. Mayle, B. P. Ruzic, and J. L. Bohn, *Phys. Rev. A* **85**, 062712 (2012).
- [47] M. Mayle, G. Quéméner, B. P. Ruzic, and J. L. Bohn, *Phys. Rev. A* **87**, 012709 (2013).
- [48] A. Christianen, M. W. Zwierlein, G. C. Groenenboom, and T. Karman, *Phys. Rev. Lett.* **123**, 123402 (2019).
- [49] P. D. Gregory, J. A. Blackmore, S. L. Bromley, and S. L. Cornish, *Phys. Rev. Lett.* **124**, 163402 (2020).
- [50] Y. Liu, M.-G. Hu, M. A. Nichols, D. D. Grimes, T. Karman, H. Guo, and K.-K. Ni, *Nat. Phys.* **16**, 1132 (2020).
- [51] M. A. Nichols, Y.-X. Liu, L. Zhu, M.-G. Hu, Y. Liu, and K.-K. Ni, *Phys. Rev. X* **12**, 011049 (2022).
- [52] M. Junker, D. Dries, C. Welford, J. Hitchcock, Y. P. Chen, and R. G. Hulet, *Phys. Rev. Lett.* **101**, 060406 (2008).
- [53] P. Pellegrini, M. Gacesa, and R. Côté, *Phys. Rev. Lett.* **101**, 053201 (2008).
- [54] See Supplemental Material at <http://link.aps.org/supplemental/10.1103/PhysRevLett.132.093403> for the details of experimental procedures and *ab initio* calculations, which includes Refs. [55–59].
- [55] H.-J. Werner, P. J. Knowles, G. Knizia, F. R. Manby, and M. Schütz, *WIREs Comput. Mol. Sci.* **2**, 242 (2012).
- [56] P. Fuentealba, H. Preuss, H. Stoll, and L. Von Szentpaly, *Chem. Phys. Lett.* **89**, 418 (1982).
- [57] P. Fuentealba, H. Stoll, L. von Szentpaly, P. Schwerdtfeger, and H. Preuss, *J. Phys. B* **16**, L323 (1983).
- [58] P. S. Żuchowski and J. M. Hutson, *Phys. Rev. A* **81**, 060703(R) (2010).
- [59] W. Müller, J. Flesch, and W. Meyer, *J. Chem. Phys.* **80**, 3297 (1984).
- [60] X.-Y. Wang, M. D. Frye, Z. Su, J. Cao, L. Liu, D.-C. Zhang, H. Yang, J. M. Hutson, B. Zhao, C.-L. Bai *et al.*, *New J. Phys.* **23**, 115010 (2021).
- [61] Z. Su, H. Yang, J. Cao, X.-Y. Wang, J. Rui, B. Zhao, and J.-W. Pan, *Phys. Rev. Lett.* **129**, 033401 (2022).
- [62] H. Yang, D.-C. Zhang, L. Liu, Y.-X. Liu, J. Nan, B. Zhao, and J.-W. Pan, *Science* **363**, 261 (2019).
- [63] H. Son, J. J. Park, Y.-K. Lu, A. O. Jamison, T. Karman, and W. Ketterle, *Science* **375**, 1006 (2022).